UDC 530.145; 530.12; 539.12-17

[1*]Nurbakova G.S., [1]Habyl N., [2]Mukushev B.A., [1]Tyulemissov Zh.Zh.

[1]Department of Physics and Technology, al-Farabi Kazakh National University, Almaty, Kazakhstan
[2]Shakarim State University, Semey, Kazakhstan
[*]e-mail: guliya_nurbakova@mail.ru

Polarization observables in rare decay $B \to K^*(\to K\pi)l^+l^-$

Abstract: Our article is devoted to the study of the $B \to K^*(\to K\pi)l^+l^-$ decay. Rare decay $B \to K^*(\to K\pi)l^+l^-$ is one of the best modes to search for new physics beyond the Standard Model (SM). A large number of observables allow for unique tests of the SM contributions.
We calculate the relevant form factors in the framework of the covariant quark model with infrared confinement in the full kinematical momentum transfer region. The calculated form factors are used to evaluate branching fractions and polarization observables in the cascade decay $B \to K^*(\to K\pi)l^+l^-$. We compare the obtained results with available experimental data and the results from other theoretical approaches. We show the relation of our helicity formalism with an approach based on the transversality amplitudes which is widely used by both experimentalists and theorists.
Key words: relativistic quark model, confinement, B-meson, rare decay, form factor, polarization observables.

Introduction

It is generally believed that the decay mode $B \to K^*(\to K\pi)\,\mu^+\mu^-$ is one of the best modes to search for new physics beyond the SM. The angular distribution makes possible an independent measurement of several observables as a function of the dilepton invariant mass. A large number of observables obtained in this manner allows for unique tests of the SM contributions [1].

The measured ratio R_K by the LHCb Collaboration [2]

$$R_K = \frac{\mathrm{B}(B^+ \to K^+\mu^+\mu^-)}{\mathrm{B}(B^+ \to K^+e^+e^-)} = \\ = 0.745^{+0.090}_{-0.074}(stat.) \pm 0.036(syst.) \qquad (1)$$

in the region $1 < q^2 < 6\ \mathrm{GeV}^2$ was found to be compatible with the SM prediction only within 2.6 standard deviations.

The results of a measurement of form-factor independent angular observables in the decay $B^0 \to K^{*0}(892)\mu^+\mu^-$ were presented in [3]. The analysis is based on a data sample corresponding to anintegrated luminosity of $1.0\,\mathrm{fb}^{-1}$, collected by the LHCb experiment in pp collisions at a center-of mass energy of 7 TeV. Four observables are measured in six bins of the dimuon invariant mass squared, q^2, in the range $0.1 < q^2 < 19.0\ \mathrm{GeV}^2$. Agreement with the SM predictions is found for 23 of the 24 measurements. A local discrepancy, corresponding to 3.7 standard deviations, is observed in one q^2 bin for one of the observables.

Our article is devoted to the study of the $B \to K^*(\to K\pi)l^+l^-$ decay. We evaluate the relevant form factors in the framework of the covariant quark model with infrared confinement. Form factors are then exploited for evaluation of physical observables.

The covariant confined quark has been applied to a large number of elementary particle processes [4, 5]. This model can be viewed as an effective quantum field approach to hadronic interactions based on an interaction Lagrangian of hadrons interacting with their constituent quarks. The coupling strength is determined by the compositeness condition $Z_H = 0$ where Z_H is the wave function renormalization constant of the hadron. The hadron field renormalization constant Z_H characterizes the overlap between the bare hadron field and the bound state formed from the constituents. Once this constant is set to zero, the dynamics of hadron interactions is fully described by constituent quarks in quark loop diagrams with

© 2016 al-Farabi Kazakh National University

local constituent quark propagators. Matrix elements are generated by a set of quark loop diagrams according to the $1/N_c$ expansion. The ultraviolet divergences of the quark loops are regularized by including vertex functions for the hadron-quark vertices which, in addition, describe finite size effects due to the non-pointlike structure of hadrons. Quark confinement was implemented into the model [6] by introducing an infrared cutoff on the upper limit of the scale integration to avoid the appearance of singularities in any matrix element. The infrared cutoff parameter λ is taken to have a common value for all processes. The covariant confined quark model contains only a few model parameters: the light and heavy constituent quark masses, the size parameters that describe the size of the distribution of the constituent quarks inside the hadron and the infrared cutoff parameter λ. They are determined by a fit to available experimental data.

Effective Lagrangian

The coupling of a meson $M\left(q_1\overline{q}_2\right)$ to its constituent quarks q_1 and $\overline{q}_2$ is described by the Lagrangian

$$L_{int}\left(x\right)=g_H M\left(x\right)\int dx_1\int dx_2 F_M\left(x,x_1,x_2\right)\overline{q}_2\left(x_2\right)\Gamma_M q_1\left(x_1\right)+h.c. \tag{2}$$

Here, Γ is a Dirac matrix which projects onto the spin quantum number of the meson field M(x). The function F_M is related to the scalar part of the Bethe-Salpeter amplitude and characterizes the finite size of the meson. To satisfy translational invariance the function F_H has to fulfil the identity $F_M\left(x+a;x_1+a,x_2+a\right)=F_M\left(x;x_1,x_2\right)$ for any four-vector a. In the following we use a specific form for the scalar vertex function

$$F_M\left(x;x_1,x_2\right)=\delta\left(x-x_1\omega_1-x_2\omega_2\right)\Phi_M\left(\left(x_1-x_2\right)^2\right), \tag{3}$$

where Φ_M is the correlation function of the two constituent quarks with masses m_{q_1}, m_{q_2} and the mass ratios $\omega_i=m_{q_i}/\left(m_{q_1}+m_{q_2}\right)$.

We choose a simple Gaussian form of the vertex function $\tilde{\Phi}_H\left(-k^2\right)$. The minus sign in the argument of this function is chosen to emphasize that we are working in the Minkowski space. One has

$$\tilde{\Phi}_H\left(-k^2\right)=exp\left(k^2/\Lambda_H^2\right) \tag{4}$$

where the parameter Λ_H characterizes the size of the meson. Since k^2 turns into $-k_E^2$ in the Euclidean space, the form (4) has the appropriate fall-off behavior in the Euclidean region. We emphasize that any choice for Φ_M is appropriate as long as it falls off sufficiently fast in the ultraviolet region of the Euclidean space to render the corresponding Feynman diagrams ultraviolet finite. We choose a Gaussian form for Φ_M for calculational convenience.

***B* – *K** form factors in the covariant quark model**

Herein our primary subject is the following matrix element, which can be expressed via dimensionless form factors:

$$\left\langle V_{[\overline{q}_1q_3]}(p_2,\varepsilon_2)\left|\,\overline{q}_2(O^\mu q_1)\,\right|P_{[\overline{q}_3q_2]}(p_1)\right\rangle = N_c g_P g_V\int\frac{d^4k}{(2\pi)^4 i}\tilde{\Phi}_P(-(k+w_{13}p_1)^2)\tilde{\Phi}_V(-(k+w_{23}p_2)^2)$$

$$\times tr\left[O^\mu S_1(k+p_1)\gamma^5 S_3(k)\not{\varepsilon}_2^\dagger S_2(k+p_2)\right]=\frac{\varepsilon_\nu^\dagger}{m_1+m_2}(-gP\cdot qA_0(q^2)+P^\mu P^\nu)A_+(q^2)+q^\mu P^\nu A_-(q^2) \tag{5}$$

$$+i\varepsilon^{\mu\nu\alpha\beta}P_\alpha q_\beta V(q^2),$$

$$\begin{aligned}
&\left\langle V_{[\bar{q}_1 q_3]}(p_2,\varepsilon_2)\,|\,\bar{q}_2(\sigma^{\mu\nu}q_\nu(1+\gamma^5))q_1)\,|\,P_{[\bar{q}_3 q_2]}(p_1)\right\rangle = \\
&= N_c g_P g_V \int \frac{d^4k}{(2\pi)^4 i}\tilde{\Phi}_P(-(k+w_{13}p_1)^2)\tilde{\Phi}_V(-(k+w_{23}p_2)^2) \\
&\times tr\left[\sigma^{\mu\nu}q_\nu(1+\gamma^5)S_1(k+p_1)\gamma^5 S_3(k)\not{\epsilon}_2^{\dagger}S_2(k+p_2)\right] \\
&= \varepsilon_\nu^{\dagger}(-(g^{\mu\nu}-q^\mu q^\nu/q^2)P\cdot q a_0(q^2)+(P^\mu P^\nu - q^\mu P^\nu P\cdot q/q^2)a_+(q^2)+i\varepsilon^{\mu\nu\alpha\beta}P_\alpha q_\beta g(q^2)).
\end{aligned} \tag{6}$$

Here, $P = p_1 + p_2$, $q = p_1 - p_2$, $\in_2^+ \cdot p_2 = 0$, $p_i^2 = m_i^2$ The form factors defined in Eq. (6) satisfy the physical requirement $a_0(0) = a_+(0)$, which ensures that no kinematic singularity appears in the matrix element at $q^2 = 0$. We will use the latest fit done in Ref. [7]. The fitted values of the constituent quark masses m_q, the infrared cut-off λ, and the size parameters Λ_H are given in Table 1.

Our form factors are represented as three-fold integrals which are calculated by using NAG routines. They are shown in Figs. 1, 2. The results of our numerical calculations are well approximated by the parametrization

$$F(q^2) = \frac{F(0)}{1 - as + bs^2}, \qquad s = \frac{q^2}{m_1^2}. \tag{7}$$

The values of $F(0)$, a and b are listed in Table 2.

Polarization observables

Let us consider the polar angle decay distribution differential in the momentum transfer squared q^2. The polar angle is defined by the angle between $\vec{q} = \vec{p}_1 - \vec{p}_2$ and $\vec{k}_1$ ($\ell^+\ell^-$ rest frame) as shown in Figure 1. One has

$$\begin{aligned}
&\frac{d^2\Gamma}{dq^2 d\cos\theta} = \frac{|\mathbf{p}_2|\upsilon}{(2\pi)^3 4m_1^3}\cdot\frac{1}{8}\sum_{pol}|M|^2 = \frac{G_F^2}{(2\pi)^3}\left(\frac{\alpha|\lambda_t|}{2\pi}\right)^2\frac{|\mathbf{p}_2|\upsilon}{8m_1^2}\times \\
&\times\frac{1}{8}\Big\{H_{11}^{\mu\nu}\cdot tr\left[\gamma_\mu\left(\not{k}_1 - m_\ell\right)\gamma_\nu\left(\not{k}_1 + m_\ell\right)\right] + H_{22}^{\mu\nu}\cdot tr\left[\gamma_\mu\gamma_5\left(\not{k}_1 - m_\ell\right)\gamma_\nu\gamma_5\left(\not{k}_1 + m_\ell\right)\right] + \\
&+H_{12}^{\mu\nu}\cdot tr\left[\gamma_\mu\left(\not{k}_1 - m_\ell\right)\gamma_\nu\gamma_5\left(\not{k}_1 + m_\ell\right)\right] + H_{21}^{\mu\nu}\cdot tr\left[\gamma_\mu\gamma_5\left(\not{k}_1 - m_\ell\right)\gamma_\nu\left(\not{k}_1 + m_\ell\right)\right]\Big\} = \\
&= \frac{G_F^2}{(2\pi)^3}\left(\frac{\alpha|\lambda_t|}{2\pi}\right)^2\frac{|\mathrm{P}_2|\upsilon}{8m_1^2}\cdot\frac{1}{2}\Big\{L_{\mu\nu}^1\cdot\left(H_{11}^{\mu\nu}+H_{22}^{\mu\nu}\right) - \\
&-\frac{1}{2}L_{\mu\nu}^2\cdot\left(q^2 H_{11}^{\mu\nu} + \left(q^2 - 4m_\ell^2\right)H_{22}^{\mu\nu}\right) + L_{\mu\nu}^3\cdot\left(H_{12}^{\mu\nu}+H_{21}^{\mu\nu}\right)\Big\},
\end{aligned} \tag{8}$$

where $|\mathbf{p}_2| = \lambda^{1/2}\left(m_1^2, m_2^2, q^2\right)/2m_1$ is the momentum of the $K(K^*)$ - meson given in the B-rest frame and $\beta_l = \sqrt{1 - 4m_l^2/q^2}$.

The differential (q2, cos θ) distribution finally reads

$$\frac{d\Gamma\left(H_1 \to H_2 \bar{\ell}\ell\right)}{dq^2 d\left(\cos\theta\right)} = \frac{3}{8}\left(1+\cos^2\theta\right)\cdot\frac{1}{2}\left(\frac{d\Gamma_U^{11}}{dq^2}+\frac{d\Gamma_U^{22}}{dq^2}\right)$$
$$+\frac{3}{4}\sin^2\theta\cdot\frac{1}{2}\left(\frac{d\Gamma_L^{11}}{dq^2}+\frac{d\Gamma_L^{22}}{dq^2}\right)-\upsilon\cdot\frac{3}{4}\cos\theta\cdot\frac{d\Gamma_P^{12}}{dq^2} \quad (9)$$
$$+\frac{3}{4}\sin^2\theta\cdot\frac{1}{2}\frac{d\tilde{\Gamma}_U^{11}}{dq^2}-\frac{3}{8}\left(1+\cos^2\theta\right)\cdot\frac{d\tilde{\Gamma}_U^{22}}{dq^2}+\frac{2}{3}\cos^2\theta\cdot\frac{1}{2}\frac{d\tilde{\Gamma}_L^{11}}{dq^2}-\frac{3}{4}\sin^2\theta\cdot\frac{1}{2}\frac{d\tilde{\Gamma}_L^{22}}{dq^2}+\frac{3}{4}\frac{d\tilde{\Gamma}_S^{22}}{dq^2}.$$

After integrating over cos θ one obtains

$$\frac{d\Gamma\left(H_1 \to H_2 \bar{\ell}\ell\right)}{dq^2} = \frac{1}{2}\left(\frac{d\Gamma_U^{11}}{dq^2}+\frac{d\Gamma_U^{22}}{dq^2}+\frac{d\Gamma_L^{11}}{dq^2}+\frac{d\Gamma_L^{22}}{dq^2}\right)+\frac{1}{2}\frac{d\tilde{\Gamma}_U^{11}}{dq^2}-\frac{d\tilde{\Gamma}_U^{22}}{dq^2}+\frac{1}{2}\frac{d\tilde{\Gamma}_L^{11}}{dq^2}-\frac{d\tilde{\Gamma}_L^{22}}{dq^2}+\frac{3}{2}\frac{d\tilde{\Gamma}_S^{22}}{dq^2}, \quad (10)$$

where the partial helicity rates $d\Gamma_X^{ij}/dq^2$ and $d\tilde{\Gamma}_X^{ij}/dq^2\ \left(X=U,L,P,S;i,j=1,2\right)$ are defined as

$$\frac{d\Gamma_{X_{ij}}}{dq^2} = \frac{G_F^2}{\left(2\pi\right)^3}\left(\frac{\alpha|\lambda_t|}{2\pi}\right)^2\frac{|\mathbf{p}_2 q^2\upsilon|}{12m_1^2}H_X^{ij}, \quad \frac{d\tilde{\Gamma}_{X_{ij}}}{dq^2} = \delta_{\ell\ell}\frac{d\Gamma_X^{ij}}{dq^2}, \quad \delta_{\ell\ell}\equiv\frac{2m_\ell^2}{q^2}. \quad (11)$$

The differential angular decay distribution in the Ref. [8] is expressed via the transversality amplitudes $A_\perp$, $A_\parallel$, A_0 and A_t. They are related to our helicity amplitudes as

$$A_\perp^{L,R} = N\frac{1}{\sqrt{2}}\left[(H_+^{(1)}-H_-^{(1)})\mp(H_+^{(2)}-H_-^{(2)})\right],$$
$$A_\parallel^{L,R} = N\frac{1}{\sqrt{2}}\left[(H_+^{(1)}+H_-^{(1)})\mp(H_+^{(2)}+H_-^{(2)})\right], \quad (12)$$
$$A_0^{L,R} = N\left[(H_0^{(1)}\mp H_0^{(2)})\right],$$
$$A_t = -2N H_t^{(2)}$$

where the overall factor is given by

$$N = \left[\frac{1}{4}\frac{G_F^2}{(2\pi)^3}\left(\frac{\alpha|\lambda_t|}{2\pi}\right)^2\frac{|\mathbf{p}_2|q^2\upsilon}{12m_1^2}\right]^{\frac{1}{2}}.$$

We do not consider here the CP-violationg observables and scalar contributions $A_S \equiv 0$. Following Ref. [9] we choose, first, three natural observables: the differential branching fraction dB/dq^2, the forward-backward asymmetry A_{FB} and the longitudinal polarization

$$\frac{d\Gamma}{dq^2} = \int d\cos\theta_l d\cos\theta_K d\phi\frac{d^4\Gamma}{dq^2\, d\cos\theta_K\, d\cos\theta_l\, d\phi} = \frac{1}{4}(3J_{1c}+6J_{1s}-J_{2c}-2J_{2s}), \quad (13)$$

$$A_{FB} = \frac{1}{d\Gamma/dq^2}\left[\int_{1-}^{0}-\int_{0}^{1}\right]d\cos\theta_l\frac{d^2\Gamma}{dq^2\, d\cos\theta_l} = -\frac{3J_{6s}}{3J_{1c}+6J_{1s}-J_{2c}-2J_{2s}}. \quad (14)$$

$$F_L = -\frac{J_{2_c}}{d\Gamma/dq^2} = \frac{1}{2}\beta_l^2\frac{H_L^{11}+H_L^{22}}{H_{tot}}. \quad (15)$$

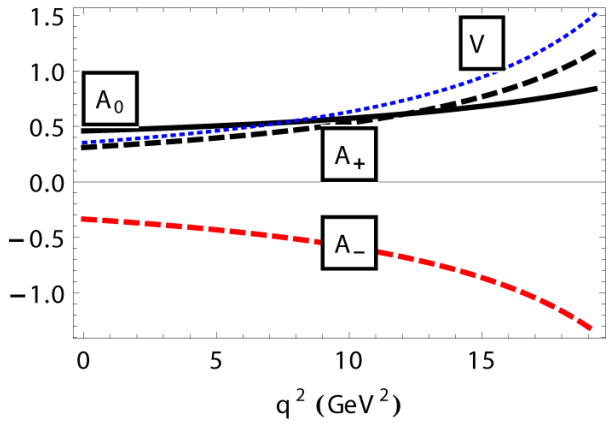

Figure 1 – The q^2-dependence of the $B - K^*$ transition V,A form factors

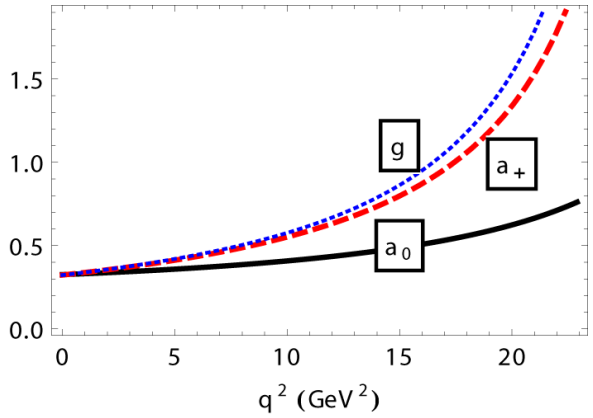

Figure 2 – The q^2-dependence of the $B - K^*$ transition T form factors

Table 1 – The fitted values of the model parameters in GeV.

$m_{u/d}$	0.241	Λ_K	1.02	Λ_{η_c}	2.06	Λ_{K^*}	0.75
m_s	0.428	Λ_D	1.71	Λ_{η_b}	2.95	Λ_{D^*}	1.51
m_c	1.67	Λ_{D_s}	1.81	Λ_ρ	0.61	$\Lambda_{D_s^*}$	1.71
m_b	5.05	Λ_B	1.96	Λ_ω	0.50	Λ_{B^*}	1.76
λ,	0.181	Λ_{B_s}	2.05	Λ_ϕ	0.91	$\Lambda_{B_s^*}$	1.71
Λ_π	0.87	Λ_{B_c}	2.50	$\Lambda_{J/\psi}$	1.93	Λ_Υ	2.96

Table 2 – Parameters for the approximated form factors in Eqs. (23) of the $B \to K^*$ transitions.

	A_0	A_+	A_-	V	a_0	a_+	G
$F(0)$	0.459	0.310	-0.335	0.354	0.326	0.323	0.323
a	0.439	1.252	1.306	1.345	0.457	1.249	1.350
b	-0.311	0.270	0.316	0.343	-0.290	0.268	0.349

Table 3 – Total branching fractions

Decay	Our	Experiments [10,12,13]
$B \to K^* \mu^+ \mu^-$	12.7×10^{-7}	$(9.24\pm0.93(stat)\pm0.67(sys))\times10^{-7}$
$B \to K^* \tau^+ \tau^-$	1.35×10^{-7}	-
$B \to K^* \gamma$	3.74×10^{-5}	$(4.21\pm0.18)\times10^{-5}$
$B \to K^* \nu\bar{\nu}$	1.36×10^{-5}	-
$B \to K \mu^+ \mu^-$	7.18×10^{-7}	$(4.29\pm0.07(stat)\pm0.21(sys))\times10^{-7}$
$B \to K \tau^+ \tau^-$	3.0×10^{-7}	-
$B \to K \nu\bar{\nu}$	0.60×10^{-5}	-

Table 4 – q^2–averages of polarization observables

	$B \to K^* l^+ l^-$							
	$< A_{FB} >$	$< F_L >$	$< P_1 >$	$< P_2 >$	$< P_3 >$	$< P_4 >$	$< P_5 >$	$< P_8 >$
μ	-0.23	0.47	-0.48	-0.31	0.0015	1.01	-0.49	-0.010
τ	-0.18	0.092	-0.74	-0.68	0.00076	1.32	-1.07	-0.0018

Conclusion

We calculate various physical observables semileptonic rare decay $B \to K^*(\to K\pi) l^+ l^-$. The values of the lepton and meson masses and the B-meson lifetime are taken from Ref. [11]. In Table 3 we give the numerical values for the total branching ratios and compare them with available experimental data. In Table 4 we give the q^2–averages of polarization observables.

Considering the outcoming numbers, it is difficult to make a clear statement about the level of agreement. Clearly, the branching fraction prediction is above both measured values. On the other hand one has to note the discrepancy which exists between the experimental values themselves and thus a question mark remains on this issue.

Acknowledgements

This work was supported by the Ministry of Education and Science of the Republic of Kazakhstan, grant 3091/GF4, state registration No. 0115RK01041.

References

1. Langenbruch C. LHCb Collaboration Latest results on rare decays from LHCb // http://arxiv.org/abs/1505.04160.

2. Aaij R. et al. LHCb Collaboration Test of lepton universality using $B^+ \to k^+ l^+ l^-$ decays // Phys. Rev. Lett. – 2014. – Vol.113. – P. 151-601.

3. Aaij R. et al. LHCb Collaboration Measurement of form-factor independent observables in the decay $B^0 \to k^{*0} \mu^+ \mu^-$ // Phys. Rev. Lett. – 2013. – Vol.111. – P. 191-801.

4. Zhaugasheva S.A., Nurbakova G.S., Saidullaeva G.G., Khabyl N. Form factors for $B \to K l^+ l^-$ decay // International Journal of mathematics and physics 5. – 2014. – No. 2. – P. 52-56.

5. Zhaugasheva S.A., Saidullaeva G.G., Nurbakova G.S., Khabyl N., Bekbaev A.K. Rare bs - decays in the covariant quark model // International Journal of mathematics and physics 5. – 2014. – No. 2. – P. 68-76.

6. Branz T., Faessler A., Gutsche T., Ivanov M. A., K¨orner J. G., Lyubovitskij V. E. Relativistic constituent quark model with infrared confinement // Phys. Rev. D – 2010. – Vol.81. – P. 034010.

7. Ganbold G., Gutsche T., Ivanov M. A. and Lyubovitskij V. E. On the meson mass spectrum in the covariant confined quark model // J. Phys. G. – 2015. – Vol.42. – P. 075002.

8. Kruger F. and Matias J. Probing New Physics Via the Transverse Amplitudes of B0-> K*0(-> K-pi+) l+l- at Large Recoil // Phys. Rev. D. – 2005. – Vol.71. – P. 094009.

9. Matias J., Mescia F., Ramon M. and Virto J. Complete Anatomy of $B \to K^* ll$ and its angular distribution // JHEP. – 2012. – Vol.1204. – P. 104.

10. Descotes–Genon S., Hurth T., Matias J. and Virto J. Optimizing the basis of $B \to K^* ll$ observables in the full kinematic range // JHEP. – 2013. – Vol.1305. – P. 137.

11. Olive K. A. et al. Particle Data Group Collaboration // Chin. Phys. C. – 2014. – Vol.38. – P. 090001.

12. Aaij R. et al. LHCb Collaboration Differential branching fractions and isospin asymmetries of $B \to K^{(*)} \mu^+ \mu^-$ decays // JHEP. – 2014. – Vol.1406. – P. 133.

13. Pescatore L. LHCb Collaboration Rare decays at the LHCb experiment // http://arxiv.org/abs/1410.2411.